



Ultrafast near-field enhancement dynamics in a resonance-mismatched nanorod excited by temporally shaped femtosecond laser double pulses

Yu Lu, Qing Yang, Feng Chen*, Guangqing Du, Yanmin Wu, Yan Ou, Xun Hou

State Key Laboratory for Manufacturing System Engineering & Key Laboratory of Photonics Technology for Information of Shaanxi Province, Xi'an Jiaotong University, Xi'an 710049, PR China

ARTICLE INFO

Article history:

Received 24 May 2015

Received in revised form

9 July 2015

Accepted 21 July 2015

Available online 29 August 2015

ABSTRACT

The spatial-temporal dynamics of the near e-field enhancement in a resonance-mismatched nanorod irradiated by the femtosecond laser double pulses is theoretically investigated. A model combining the non-equilibrium electron excitation dynamics and the near field scattering was built for well exploring ultrafast dynamics of the e-field enhancement around the nanorod. It is revealed that the average enhancement factor can be evidently improved with increasing the double pulses separation. The energy ratio of the temporally shaped double pulses with respect to the highest enhancement factor shows an evident decrease with the increasing the total laser fluence. In addition, the most evident promotion of average enhancement factor from 51.2 to 78.8 can be acquired under laser fluence of $0.7F_{th}$, which could be attributed to the temperature modulation of electron states excited by the temporally shaped double pulses. The study provides the base for understanding ultrafast plasmon dynamics for advancing the applications such as fs super-resolution fabrication, fs near field imaging and the generation of ultrashort extreme-ultraviolet pulses.

© 2015 Elsevier Ltd. All rights reserved.

1. Introduction

Giant electric field enhancement near the metallic nanostructures has shown significant potentials in the fields such as super-resolution fabrication and imaging, single molecular fluorescence and the generation of ultrashort extreme-ultraviolet pulses [1–3]. The enhanced electric field associated with localized surface plasmon resonances (LSPRs) has been demonstrated to be dependent on the size, geometry as well as the optical properties of nano-structures [4–6]. Most of the previous works has been made on promoting the near field enhancement via tuning geometries of nanostructures such as the nanostructures' shape, size and the gap distance [7,8]. Unfortunately, hugely enhanced e-field could usually be impaired by resonance mismatching, which originates from the geometry deviation of the nanostructure to the ideal one during the synthesis and fabrication process [9–11]. In order to advance the near-field applications, highly precise fabrication of the nanostructures such as e-beam lithography is required [12,13], which is at the cost of the complexity of the procedures. As

a result, an alternative route for promoting near-field enhancement in mismatched nanostructures, which does not depend on the highly precise synthesis and fabrication, is highly desirable.

Recently, the temporally shaped femtosecond laser excitation, namely, multi-pulse sequence with variable temporal separation has stimulated great interests in tuning the material excitation for a wide range of applications [14–16]. Considering that the dielectric constants of metallic materials, $\epsilon_m(\omega, T_e)$, depend much on the excited electrons according to Drude model [17,18], great opportunities exist that the transient behavior of the plasmon resonance for mismatched nanostructures can be promoted via tuning the parameters of the temporally shaped pulses such as pulse separation and pulse energy ratio. Take the temporally shaped double pulses for example, when irradiated by the first femtosecond laser pulse, the free electrons in metallic materials can be excited to nearly 1 eV in femtosecond scale, leading to evident modification of the optical properties of nanostructures. The separation of the temporally shaped pulses can be tuned in the tens or hundreds of femtoseconds, which is much shorter than the time scale of the electron thermal relaxation. So before irradiated by the second pulse, the optical properties of the metallic nanostructures has been dramatically modified by the former pulse due to the highly excited electrons. Consequently, the

* Corresponding author.

E-mail addresses: chenfeng@mail.xjtu.edu.cn (F. Chen), guangqingdu@mail.xjtu.edu.cn (G. Du).

plasmon excited by the second pulse would be modulated by the former one to a large extent due to the pulse-to-pulse correlation. The effectiveness of the modulation of surface plasmon resonance on the surface of metallic or electron-excited dielectric films has been proved by the previous works [19–21]. However, the thermal dynamics manipulation of the enhanced near-field in metallic 2D or 3D nanostructures via temporally shaped femtosecond pulses is still an undeveloped topic.

In this paper, the ultrafast dynamics for manipulation of near-field enhancements on a resonance mismatched nanorod via temporally shaped femtosecond laser was theoretically investigated.

2. Models and methods

When a gold nanorod is irradiated by the temporally shaped femtosecond pulses, the electron system of the nanorods is initially excited by the pre-pulse. Synchronously the optical properties on the thermal excitation zone could be effectively tuned via modifying the electron state distribution. After that, the second pulse will interact with the nanorod excited by the pre-pulse, leading to the modifications of the e-field enhancement on the excitation zones. The near field enhancement highly depends on the thermally excited electrons due to the modified dielectric constants. Consequently, the transient enhanced e-field $E(t)$ is affected by the transient electron temperature $T_e(t)$ for a given incident wavelength due to the interaction of temporally shaped pulses on the nanorod. The near field enhancement varying with the incident wavelength and the electron temperature, $\eta(\epsilon_m(\omega, T_e))$, is investigated based on the finite element method (FEM). The exact expression and value of dielectric constant of the Au nanorod $\epsilon_m(\omega, T_e)$ is shown in Ref. [17]. The detail will be shown in the “results and discussion” section. In addition, the electron thermal dynamics during the ultrafast interaction process should also be taken into consideration, in which the electrons and phonons should be regarded as respective systems. As a result, the electron thermal dynamics can be described by the two-temperature model (TTM):

$$\begin{aligned} C_e(T_e) \frac{\partial T_e}{\partial t} &= g \cdot (T_p - T_e) + S(t) \\ C_p(T_p) \frac{\partial T_p}{\partial t} &= g \cdot (T_e - T_p) \end{aligned} \quad (1)$$

In the equation set, T_e and T_p are electron and photon temperature, $C_e(T_e)$ and $C_p(T_p)$ are the thermal capacity of electrons and photons and g is the electron–phonon coupling strength. The exact value of the parameters in equation set (1) has been shown in the Ref. [16]. In TTM equation set used in our model, the thermal conductivity terms are reasonably omitted because the temperature distribution at various time can be regarded as a constant in the nanorod and $\nabla(k_e \nabla T_e)$ or $\nabla(k_p \nabla T_p)$ is ignorable according to related experimental and theoretical results shown in Ref. [22–24]. $S(t)$ is the absorbed laser fluence given by

$$S(t) = \frac{C_{abs}(t) \cdot F_{SPT}(t)}{V_{rod}} \quad (2)$$

where $C_{abs}(t)$ is the absorbing cross section, which can be numerically acquired in our simulation, and V_{rod} is the volume of the nanorod. The temporally fluence intensity of the shaped double pulses, $F_{SPT}(t)$, is described by multi-Gaussian profile:

$$\begin{aligned} F_{SPT}(t) &= \sum_{i=1,2} F_i \cdot \tau_i(t) = \sqrt{\frac{4 \ln 2}{\pi}} \\ &\cdot \sum_i \frac{F_i}{t_p} \cdot \exp\left(-4 \ln 2 \cdot \left(\frac{t - 2t_p - t_i}{t_p}\right)^2\right) \end{aligned} \quad (3)$$

in which F_i is the laser fluence of respective pulses of temporally shaped pulses sequence and the FWHM pulse duration is t_p 65 fs in our model. The time-dependent electric field strength $E(t)$ will be modulated by both the intensity profile of the laser pulse and the transient electron temperature. Considering the fact that the relaxation time of the plasmon is as short as several fs [25–27], it is reasonable to assume that the e-field response to incident laser pulse can be treated as a constant delay of a few femtoseconds. However, the temporal shape of the e-field enhancement can be affected less with respect to the response delay. As a result, the temporal e-field strength can be written as

$$E(t) = \eta(\epsilon_m(\omega, T_e)) \cdot E_{inc}(t) \quad (4)$$

in which $\eta(\epsilon_m(\omega, T_e))$ is the temporal e-field enhancement factor decided by the transient electron temperature as well as the incident wavelength and $E_{inc}(t)$ is the strength of the incident e-field. To measure the electric field enhancement effect in the whole laser pulse duration, a normalized average enhancement factor η_{ave} modulated by the shape of the laser is induced:

$$\eta_{ave} = \frac{\int E(t) dt}{E_0 \cdot t_p} \quad (5)$$

In the equation, $E(t)$ the temporally e-field strength at the detecting point and E_0 is the peak electric field of the threshold fluence (F_{th}) for the nanorods' size reducing or ablation due to the thermal effect defined in Ref. [22]. The typical shaped double femtosecond pulses are considered in the current simulations.

3. Results and discussions

The e-field enhancement spectrum with respect to the electron temperature modifications is shown in Fig. 1(b). The enhanced e-field of more than 100 times of the incident light can be acquired by modulating the electron temperature when the wavelength varies from 800 nm to 900 nm, a resonance wavelength range supported by the related experimental results [28,29]. For incident laser with wavelength of 800 nm applied in our simulation, the nanorod is a resonance-mismatched structure at room temperature under which the resonance wavelength is 850 nm. When the electron temperature varies from 300 K to 3000 K, the resonance wavelength has a decrease with increasing electron temperature, gradually approaching to the incident wavelength 800 nm. As a result, the enhancement factor under 800 nm incident light also increases from 60 to 100. With the electron temperature over 5000 K, however, the enhancement factor decreases so evidently that the enhancement factor is even much lower than that in room temperature due to the over excited electrons. The results indicate that the e-field at the end of the nanorod is more effectively concentrated and enhanced when the electron is moderately excited. The most sufficiently enhancement can be acquired when the electron temperature is 3000 K and the electron temperature over 5000 K leads to low-efficiency amplification. As a result, it is reasonable that the near field can be advanced via modulating the electron thermal dynamics.

The average enhancement factor η_{ave} varying with pulse separation of the temporally shaped double pulses is shown in Fig. 2. The average enhancement factors increase evidently compared with the single pulse containing the same total fluence

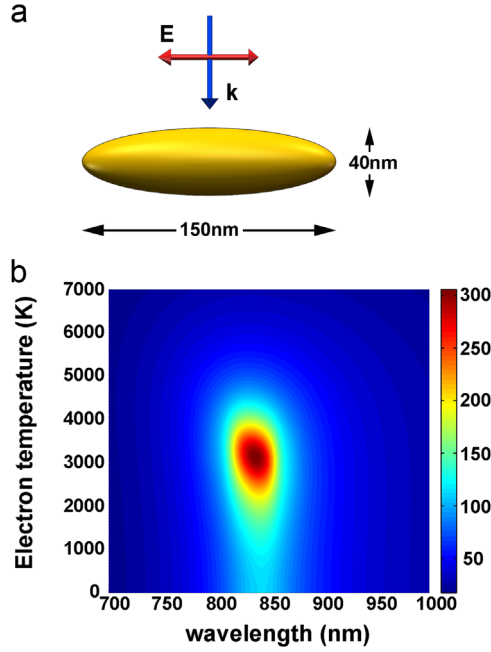


Fig.1. (a) Scheme of the model: the size of the nanorod, the direction and polarization of the incident laser. The nanorod is 150 nm in the long-axis with an aspect of 3.75. The detecting point is 2 nm to the end of the nanorod and the polarization is along the long axis of the nanorod. The media is water with the refractive index of 1.33. (b) Enhancement factor $\eta(\epsilon_m(\omega, T_e))$ at the detection point depending on incident wavelength and the electron temperature.

(corresponding to the double pulses with the separation time of 0). When the pulse separation time is 0 fs, the enhancement factors are 48.0, 49.5, 50.5 and 51.2 with the laser fluence of $0.4F_{th}$, $0.5F_{th}$, $0.6F_{th}$, and $0.7F_{th}$. When the separation time is 200 fs, however, the highest enhancement factors under fluence of $0.4F_{th}$,

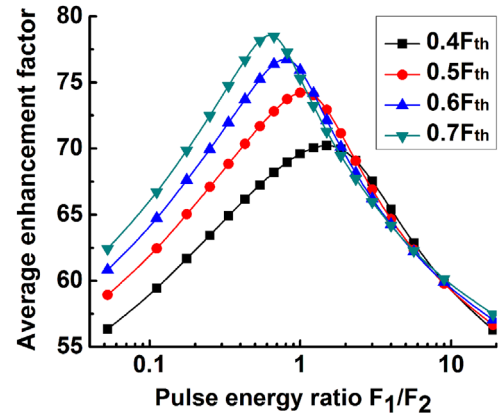


Fig.3. The average enhancement factor depending on the variation of energy pulse ratio under the pulse fluence of $0.4F_{th}$, $0.5F_{th}$, $0.6F_{th}$, and $0.7F_{th}$.

$0.5F_{th}$, $0.6F_{th}$, and $0.7F_{th}$ could be improved to 70.0, 74.0, 76.8 and 78.8, respectively. For single pulses, all the energy is concentrated in single pulse duration and the electrons will be sharply heated to high temperature more than 5000 K, under which the near field enhancement factor $\eta(\epsilon_m(\omega, T_e))$ will decrease rapidly. As a result, the laser pulse could not be amplified sufficiently because electron is over excited when irradiated by a single pulse with high fluence. When the shaped pulses train is applied, the electron thermal-dynamic process can be modified by the pulse-to-pulse interaction. As a consequence, the electron exciting process could be decelerated and the over excited states of the electrons could be avoided to a large extent, leading to the sufficient application of the laser fluence. The results indicate that the electron dynamics in nanorod can be evidently modulated by tuning the pulse separation of the temporally shaped doubles. Tuning the separation time of the temporal shaped pulse could affect the electron dynamics through decelerating the electron heating process, which

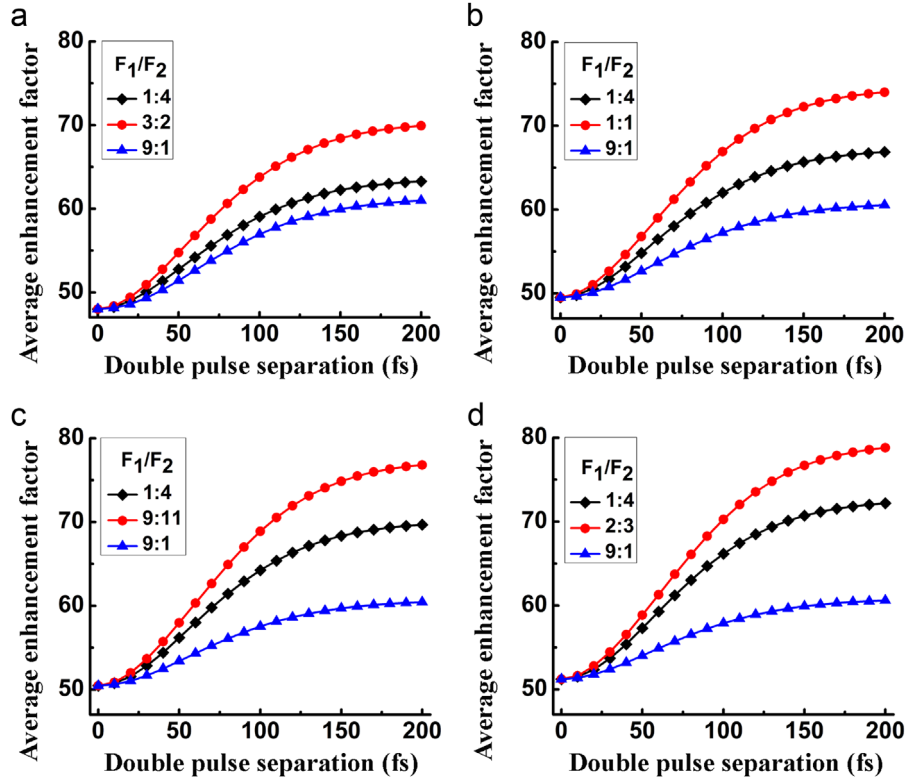


Fig.2. The average enhancement factor depending on the separation time and energy ratio (F_1/F_2) under total laser fluence of (a) $0.4F_{th}$, (b) $0.5F_{th}$, (c) $0.6F_{th}$ and (d) $0.7F_{th}$.

will improve the efficiency of the e-field amplification in femto-second scale.

Fig. 3 shows the relationship between average enhancement factor and the energy ratio of the first and second pulse (F_1/F_2). The separation time of the two pulses is selected to be 200 fs. It shows that the average enhancement factor can be evidently modified by tuning the energy ratio of the two pulses. With the pulse energy ratio of 1:19, the average enhancement factor is 56.3, 58.9, 60.8 and 62.4 at the laser fluence of $0.4F_{th}$, $0.5F_{th}$, $0.6F_{th}$ and $0.7F_{th}$, respectively. With the pulse energy ratio of 19:1, the average enhancement factor is 56.3, 56.7, 57.0 and 57.5 at the laser fluence of $0.4F_{th}$, $0.5F_{th}$, $0.6F_{th}$ and $0.7F_{th}$, respectively. The slight improvement of average enhancement factor can be attributed to the failure of the tuning of the electron dynamics in the nanorod. An extreme energy ratio of the double pulses will lead to an insufficient amplification of the incident laser due to the less or over excitation of electrons. The highest enhancement factor of 70.0, 74.0 and 76.8 can be reached at the fluence of $0.4F_{th}$, $0.5F_{th}$ and $0.6F_{th}$ with optimal energy ratio of 3:2, 1:1 and 9:11, respectively. The most evident promotion of the average enhancement factor from 51.2 to 78.8 exists when the fluence is $0.7F_{th}$ and pulse energy ratio is 2:3. The optimal average enhancement factor can be acquired when the energy of the first pulse is controlled at $0.26F_{th}$, indicating that electron temperature plays a key role in the transient behavior of electric field strength. The free electrons in nanorod can be excited to the state with electron temperature at 3000 K by the first pulse, under which the quasi-resonance state can be achieved. As a result, the most sufficient amplification of the laser fluence can be acquired according to the prediction shown in Fig. 1.

The spatio-temporal evolution of the electric field under different double pulse energy ratio is shown in Fig. 4. It shows that the electric field presents a prominent decay with the distance to the end of the nanorod increasing (shown in the insert picture in Fig. 4(a)). When the distance reaches to about 20 nm, the electric field become ignorable compared with the field near the end, indicating that the majority of the pulse energy concentrates in a domain much smaller than the diffraction limiting scale. The

temporal evolution of the electric field under different pulse energy ratio is also shown in Fig. 4. It can be seen from Fig. 4(a) that it exhibits the highest transient enhancement of 130 for a single femtosecond pulse. When irradiated by the single pulse, the electrons of the nanorod can be excited to the 3000 K so sharply that the electric field can reach to the peak strength soon. On the other hand, however, the near field electric strength decreases fast as soon as it reaches the peak strength due to the rapidly increasing electron temperature. As a result, the average enhancement factor of a single pulse is not very high because of the over excited electrons. For the double pulses with the energy ratio of 9:1 shown in Fig. 4(b), the strongest e-field in the first pulse is 125 and the second pulse is weak because the electrons in the rod have been over excited by the first pulse. When the energy ratio is 1:4 shown in Fig. 4(d), the e-field excited by the first pulse is not strong due to the failure of achieving the optimized enhancement temperature. The e-field excited by the second pulse could be amplified to as high as 105. Fig 4(c) shows the the spatio-temporal profile of e-field with the energy ratio of 2:3. It can be seen from the figure that both of the pulses have been amplified sufficiently and the peak electric strength excited by the two pulses respectively are about 70 and 65. For the separated double pulses, although the peak electric field is not as strong as that of a single pulse because in shaped double pulses the total energy is separated into two parts, a longer interaction time makes the average enhancement factor eventually higher than the enhancement factor of a single pulse.

4. Conclusion

In conclusion, the ultrafast dynamics of the e-field enhancement at a gold nanorod has been theoretically investigated. The average e-field enhancement factor in a mismatching structure nanorod can be evidently promoted via the temporally shaped double sequence. The average enhancement factor can be evidently promoted through increasing the separation time between the double pulses, indicating that the decelerating of the electron

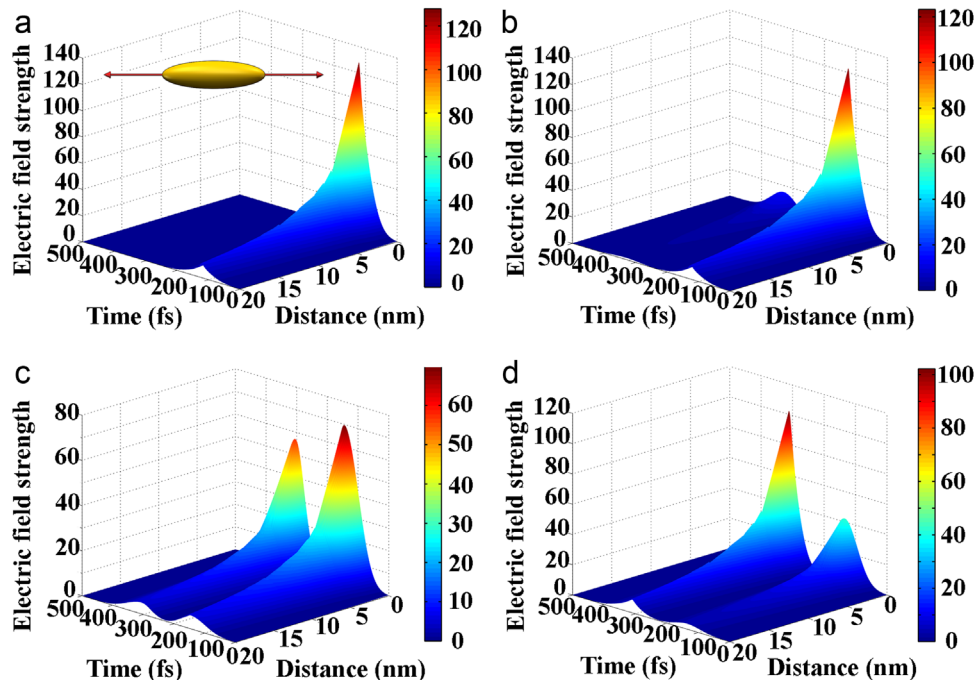


Fig. 4. The spatio-temporal evolution of the e-field along the axis (shown in insert picture of the Fig. 4(a)) of the nanorod under energy ratio of (a) single pulse (b) 9:1 (c) 2:3 (d) 1:4. The total energy is $0.7F_{th}$ and the separation time is 200 fs. The “distance axis” refers to the distance from the detecting point to the end of nanorod.

heating process would lead to more sufficient amplification of the laser in the near field. Over 50 percent improvement of the average enhancement factor can be acquired with the double pulse energy ratio of 3:2, 1:1 and 9:11 under the laser fluence of $0.4F_{th}$, $0.5F_{th}$ and $0.6F_{th}$, respectively. The most evident promotion of the near field enhancement is acquired when the laser fluence is $0.7F_{th}$, at which the average enhancement factor can be promoted from 51.2 to 78.7 with the pulse energy ratio of 2:3. The result also indicates that the fluence in the first pulse of $0.26F_{th}$ plays a key role in acquiring the highest average enhancement factor at which the electrons could be excited to the quasi-resonance state of 3000 K. The research shows a flexible method with multi-tunable degrees of freedom to optimize the e-field strength in femtosecond scale, which shows potential in applications such as super-resolution fabrication and extreme-ultraviolet light sources.

Acknowledgment

This work is supported by the National Natural Science Foundation of China under Grant nos. 51335008, 61275008 and 11404254, and the specially funded program on national key scientific instruments and equipment development of China under Grant no. 2012YQ12004706, the Collaborative Innovation Center of high-end Manufacturing Equipment.

Reference

- [1] B. Simkhovich, G. Bartal, Plasmon-enhanced four-wave mixing for super-resolution applications, *Phys. Rev. Lett.* 112 (2014) 056802.
- [2] A. Kinkhabwala, Z. Yu, S. Fan, Y. Avlasevich, K. Müllen, W.E. Moerner, Large single-molecule, *Nat. Photonics* 3 (2009) 654–657.
- [3] I. Park, S. Kim, J. Choi, D.H. Lee, Y.J. Kim, M.F. Kling, M.I. Stockman, S.W. Kim, Plasmonic generation of ultrashort extreme-ultraviolet light pulses, *Nat. Photonics* 5 (2011) 677–681.
- [4] F. Minkowski, F. Wang, A. Chakrabarty, Q. Wei, Resonant cavity modes of circular plasmonic patch nanoantennas, *Appl. Phys. Lett.* 104 (2014) 021111.
- [5] W. Ni, X. Kou, Z. Yang, J. Wang, Tailoring longitudinal surface plasmon wavelengths, scattering and absorption cross sections of gold nanorods, *ACS Nano* 6 (2012) 677–686.
- [6] K.C. Woo, L. Shao, H. Chen, Y. Liang, J. Wang, H.Q. Lin, Universal scaling and Fano resonance in the plasmon coupling between gold nanorods, *ACS Nano* 5 (2011) 5976–5986.
- [7] T. Søndergaard, S.I. Bozhevolnyi, J. Beermann, S.M. Novikov, E. Devaux, T. W. Ebbesen, Resonant plasmon nanofocusing by closed tapered gaps, *Nano Lett.* 10 (2010) 291–295.
- [8] W. Ding, R. Bachelot, S. Kostcheev, P. Royer, R.E. de Lamaestre, Surface plasmon resonances in silver Bowtie nanoantennas with varied bow angles, *J. Appl. Phys.* 108 (2010) 124314.
- [9] S.E. Lohse, C.J. Murphy, The quest for shape control: a history of gold nanorod synthesis, *Chem. Mater.* 25 (2013) 1250–1261.
- [10] M.R.K. Ali, B. Snyder, M.A. El-Sayed, Synthesis and optical properties of small Au nanorods using a seedless growth technique, *Langmuir* 28 (2012) 9807–9815.
- [11] L. Vigdeman, E.R. Zubarev, High-yield synthesis of gold nanorods with longitudinal SPR peak greater than 1200 nm using hydroquinone as a reducing agent, *Chem. Mater.* 25 (2013) 1450–1457.
- [12] W. Zhang, L. Huang, C. Santschi, O.J.F. Martin, Trapping and sensing 10 nm metal nanoparticles using plasmonic dipole antennas, *Nano Lett.* 10 (2010) 1006–1011.
- [13] N.A. Hatab, C.H. Hsueh, A.L. Gaddis, S.T. Retterer, J.H. Li, G. Eres, Z. Zhang, B. Gu, Free-standing optical gold bowtie nanoantenna with variable gap size for enhanced Raman spectroscopy, *Nano Lett.* 10 (2010) 4952–4955.
- [14] K.F. MacDonald, Z.L. Samsen, M.I. Stockman, N.I. Zheludev, Ultrafast active plasmonics, *Nat. Photonics* 3 (2009) 55–58.
- [15] F. Zhang, Xi. Hu, Y. Zhu, Y. Fu, H. Yang, Q. Gong, Ultrafast all-optical tunable Fano resonance in nonlinear metamaterials, *Appl. Phys. Lett.* 102 (2013) 181109.
- [16] G. Du, F. Chen, Q. Yang, J. Si, X. Hou, Ultrafast thermalization characteristics in Au film irradiated by temporally shaped femtosecond laser pulses, *Opt. Commun.* 284 (2011) 640–645.
- [17] J. Hsu, C. Fuentes-Hernandez, A.R. Ernst, J.M. Hales, J.W. Perry, B. Kippelen, Linear and nonlinear optical properties of Ag/Au bilayer thin films, *Opt. Express* 20 (2012) 8629–8640.
- [18] G. Du, Q. Yang, F. Chen, J. Si, X. Hou, Insight into the thermionic emission regimes under gold film thermal relaxation excited by a femtosecond pulse, *Appl. Surf. Sci.* 257 (2011) 9177–9182.
- [19] G. Du, F. Chen, Q. Yang, Y. Ou, Y. Wu, Y. Lu, H. Bian, X. Hou, Ultrafast dynamics of high-contrast nano-grating formation on gold film induced by temporally shaped femtosecond laser, *Chem. Phys. Lett.* 597 (2014) 153–157.
- [20] G. Du, Q. Yang, F. Chen, H. Bian, X. Meng, J. Si, F. Yun, X. Hou, Ultrafast electron dynamics manipulation of laser induced periodic ripples via a train of shaped pulses, *Laser Phys. Lett.* 10 (2013) 026003.
- [21] R. Stoian, M. Boyle, A. Thoss, A. Rosenfeld, G. Korn, I.V. Hertel, E.E.B. Campbell, Laser ablation of dielectrics with temporally shaped femtosecond pulses, *Appl. Phys. Lett.* 80 (2002) 353.
- [22] O. Warshavski, Li Minal, G. Bisker, D. Yelin, Effect of single femtosecond pulses on gold nanoparticles, *J. Phys. Chem. C* 115 (2011) 3910–3917.
- [23] K. Setoura, D. Werner, S. Hashimoto, Optical scattering spectral thermometry and refractometry of a single gold nanoparticle under CW Laser excitation, *J. Phys. Chem. C* 116 (2012) 15458–15466.
- [24] G. Baffou, H. Rigneault, Femtosecond-pulsed optical heating of gold nanoparticles, *Phys. Rev. B* 84 (2011) 035415.
- [25] I.D. Mayergoyz, Z. Zhang, G. Miano, Ultrafast temperature relaxation evolution in Au film under femtosecond laser pulses irradiation, *Phys. Rev. Lett.* 98 (2007) 147401.
- [26] A. Anderson, K.S. Deryckx, X.G. Xu, G. Steinmeyer, M.B. Raschke, Few-femtosecond plasmon dephasing of a single metallic nanostructure from optical response function reconstruction by interferometric frequency resolved optical gating, *Nano Lett.* 10 (2010) 2519–2524.
- [27] T. Hanke, G. Krauss, D. Trautlein, B. Wild, R. Bratschitsch, A. Leitenstorfer, *Phys. Rev. Lett.* 103 (2009) 257404.
- [28] Jorge Pérez-Juste, Isabel Pastoriza-Santos, Luis M. Liz-Marzán, Paul Mulvaney, Coordin. Shape control in gold nanoparticle synthesis, *Chem. Rev.* 249 (2005) 1870–1901.
- [29] P.K. Jain, K.S. Lee, I.H. El-Sayed, M.A. El-Sayed, Calculated absorption and scattering properties of gold nanoparticles of different size, shape, and composition: applications in biological imaging and biomedicine, *J. Phys. Chem. B* 110 (2006) 7238–7248.